Title
Interaction of a rotational relativistic electron beam with a magnetized plasma

Journal
Physics of Fluids, 17(4)

ISSN
00319171

Author
Chu, K. R

Publication Date
1974

DOI
10.1063/1.1694794

Peer reviewed

Interaction of a rotational relativistic electron beam with a magnetized plasma

K. R. Chu* and N. Rostoker†

Laboratory of Plasma Studies and School of Applied and Engineering Physics, Cornell University, Ithaca, New York 14850

(Received 31 January 1973; final manuscript received 30 November 1973)

In the presence of a uniform magnetic field, it is possible to form a hollow rotational relativistic electron beam which gyrates as a whole about its axis while propagating axially along the magnetic field. Here, the interaction of a rotational beam front with a dense magnetized plasma is studied. Starting from the two-fluid equations for the plasma, it is shown that under the conditions $a_2 - a_1 \gg \lambda$, $\Omega_e \gg \nu_e$, and $\Omega_i \ll \nu_i$, where $a_2 - a_1$ is the beam thickness, λ is the plasma skin depth, Ω is the gyro frequency, and ν is the momentum transfer collision frequency, the beam current will not only be axially neutralized as usual but also angularly neutralized by a *drift* plasma current. The subsequent decay of these counter currents will in return induce upon the beam an *axial* retarding force capable of dissipating most of the beam axial energy in a few nsec. In addition to Ohmic heating the plasma electrons, a significant portion of the beam axial energy lost in the above manner will be transformed into ion energies through the action of a current sustained radial electrostatic field. Possible applications to plasma heating and beam trapping in astron type machines are discussed.

I. INTRODUCTION

In recent years, the development of high voltage pulsed electron generators made it possible to produce intense relativistic electron beams with current up to 2 MA and electron energy up to 15 MeV. The beam pulse contains total energy up to many megaJoules and lasts from 50 to 100 nsec.

Besides the obvious problem of beam generation, the main concern during the early phase of the development was for the propagational properties of the beam inside a pre-ionized or beam-generated plasma. Theoretical results[1-8] on beam propagation have been in general agreement with the experiments.[9-16]

Recently, the beam programs have been diversified into various areas of thermonuclear fusion-oriented applications. For example, the high current of the beam may be used for magnetic field shaping in confinement devices such as the astron on the one hand,[17-19] and the intense energy density of the beam may be used for plasma heating on the other.

Confining our attention to the two areas of applications outlined above, we find it to be of theoretical as well as practical interest to study the interaction of a hollow, cylindrical, and rotational relativistic electron beam with a magnetized background plasma. By a rotational beam, we mean that each beam electron, in addition to its propagation velocity, is gyrating about the beam axis under the influence of an axial applied magnetic field. This model can be realized by, for example,

i. injecting an electron beam at nearly right angles into a uniform magnetic field.[19] Each beam electron so injected will follow a helical orbit with short pitch distances. As a result of the continuous injection and the inevitable beam velocity spread, the electrons will superimpose into a hollow rotational beam as our model describes, or

ii. passing a nonrotational hollow electron beam through an axially symmetric cusp magnetic field. The beam will thus gain a rotational velocity through the $J_{bz} \times B_r$ force, where J_{bz} is the beam axial current density and B_r is the radial cusp magnetic field. A detailed description of this method can be found elsewhere.[20,21]

In the astron experments, a primary step is to trap a rotational electron beam in the magnetic mirror configuration to form the E layer. Difficulty arises because the electrons do not easily get trapped as the simple adiabatic theory has predicted. A method that has been used to improve trapping efficiency is to surround the beam path with resistive rings.[22] Nebenzahl[23] has shown that the energy dissipated in the rings by the beam induced ring currents is at the cost of beam axial energy, while the rotational velocity of the beam remains unchanged. As a result, the beam may be slowed down considerably on its way to the magnetic mirror end, with an increased probability of being reflected back.

However, this method would not work if there is a dense plasma present, since the beam can no longer interact with the external rings when shielded by a dense plasma. Under such conditions, it would be highly desirable to have the plasma, a resistive medium itself, serve the purpose of the rings. In this paper, such a trapping scheme is studied. Assuming $\Omega_e \gg \nu_e$, $\Omega_i \ll \nu_i$, and $a_2 - a_1 \gg \lambda$, we will show that the beam currents (axial and angular) will be fully neutralized by counter flowing plasma currents whose subsequent decay can indeed produce an efficient retarding force on the beam. To parallel the resistive ring trapping method further, all the energy dissipated by the plasma counter currents is at the cost of the beam axial energy alone.

As a consequence of the enormous beam axial energy release during its retardation stage, significant plasma heating will take place. This is perhaps a potentially more important aspect of the whole scheme, because not only the plasma electrons will be Ohmic heated by the counter

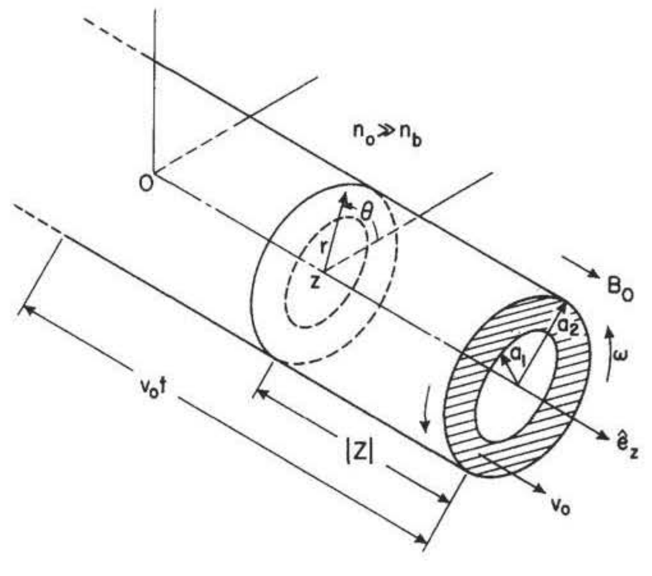

FIG. 1. A hollow rotational relativistic electron beam propagating in a dense magnetized plasma.

currents, but the ions will also be heated by a persistent space charge electric field required to sustain the angular counter current. It should be pointed out that in the heating process the plasma counter currents carry very little energy of their own. They essentially serve as "channels" through which the beam could strongly interact with the plasma. This is comparable to a heating mechanism proposed by Lovelace and Sudan[24] in connection with a nonrotational relativistic electron beam. In their proposal, the beam-induced plasma counter current also plays a similar role. However, there is a major difference in the way ions are heated. In Lovelace and Sudan's case, ion heating is due to ion sound turbulence. In the present case, the ions are electrostatically heated.

We will now turn to the theoretical aspects of the problem and look at some new complications introduced by the rotational motion of the beam.

In most of the earlier treatments of electron beam and plasma interactions, the electron dynamics of the plasma have been the main concern, while ions were assumed to be stationary. The same treatment will not be adequate here for the following reason. We will soon show that the angular counter current, which flows perpendicular to the applied magnetic field, is carried by drifting electrons. Therefore, there exists a radial space charge electric field to provide the $E \times B$ electron drift velocity. Under this electric field, ions will no longer be stationary, therefore consideration of ion dynamics becomes essential.

Furthermore, the formation of an angular counter current also depends crucially on the collisional effects of the plasma particles, since, in the absence of collisions, the orbit theory states that the $E \times B$ drift velocities of ions and electrons are equal and in the same direction, and thus add up to zero net drift current.

In Sec. II, the model and mathematical formulation are presented. In Sec. III, under the assumptions $\Omega_e \gg \nu_e$ and $\Omega_i \ll \nu_i$, analytic solutions are obtained through a series of expansions. In Sec. IV, counter currents and their decay mechanisms are discussed. In Sec. V, a strong axial retarding force on the beam is shown to result from the decay of counter currents (the angular one in particular). Its significance for the trapping of the beam into an astron type machine is considered. In Sec. VI, plasma heating and detailed energy transfer processes are discussed. We show that the total energy is conserved.

II. MODEL AND FORMULATION

Our model as depicted in Fig. 1 consists of the following: Inside a uniformly magnetized plasma ($\mathbf{B} = B_0\hat{e}_z$), a hollow cylindrical relativistic electron beam, whose axis coincides with the z axis, is rotating rigidly ($v_{b\theta} = r\omega$) and propagating axially with a constant velocity $v_0\hat{e}_z$. We assume (i) that the beam is semi-infinite and of uniform density; (ii) that each individual beam electron is gyrating independently about the beam axis so that $\omega \approx eB_0/(\gamma mc)$, where γ is the average relativistic factor of the beam electrons; (iii) that the plasma density is $10^{12}/\text{cm}^3$ or more and much denser than the beam; and (iv) that the system is at a steady state in the frame for which the beam has no axial velocity.

The semi-infinite beam model is conveniently extendable to a finite length one since the latter can be modeled by superimposing two semi-infinite beams of opposite charges.

In setting up the model, we have virtually assumed that the beam motion will not be disturbed by its own fields or those due to the plasma. This assumption will prove to be self-consistent with we show a posteriori that the beam would be both charge and current neutralized.

Our main effort is to find the responses of the plasma to beam penetration and their effects as produced back on the beam. Except for a few changes, the formulation presented here is similar to our previous paper.[8] We describe the plasma dynamics by the cold plasma two-fluid equations

$$\frac{\partial \mathbf{v}_e}{\partial t} + (\mathbf{v}_e \cdot \nabla)\mathbf{v}_e = -\frac{e}{m}\left(\mathbf{E} + \frac{1}{c}\mathbf{v}_e \times \mathbf{B}\right) - \nu_e \mathbf{v}_e, \quad (1)$$

$$\frac{\partial \mathbf{v}_i}{\partial t} + (\mathbf{v}_i \cdot \nabla)\mathbf{v}_i = \frac{e}{M}\left(\mathbf{E} + \frac{1}{c}\mathbf{v}_i \times \mathbf{B}\right) - \nu_i \mathbf{v}_i, \quad (2)$$

where a phenomenological momentum relaxation term is added to each equation, and m is the electron mass, M is the ion mass, ν_e is the electron momentum transfer collision frequency, and ν_i is the ion momentum transfer collision frequency.

By virtue of assumption (iv), we can combine t and z into one variable by defining $Z = z - v_0 t$, where $|Z|$ is the distance from z to the beam front.

Substituting $\partial/\partial z$ by $\partial/\partial Z$, and $\partial/\partial t$ by $-v_0\partial/\partial Z$ into Eqs. (1) and (2), linearizing and Fourier transforming the resulting equations, we obtain

$$(-s + \nu_e)\delta\mathbf{v}_e(\mathbf{k}) = -(e/m)\delta\mathbf{E}(\mathbf{k}) - \Omega_e \delta\mathbf{v}_e \times \hat{e}_z \quad (3)$$

$$(-s + \nu_i)\delta\mathbf{v}_i(\mathbf{k}) = (e/M)\delta\mathbf{E}(\mathbf{k}) + \Omega_i \delta\mathbf{v}_i \times \hat{e}_z, \quad (4)$$

where $\Omega_e = eB_0/(mc)$, $\Omega_i = eB_0/(Mc)$, and we have defined $s = ik_z v_0$ for simplicity.

For later convenience, we introduce a new frame (see

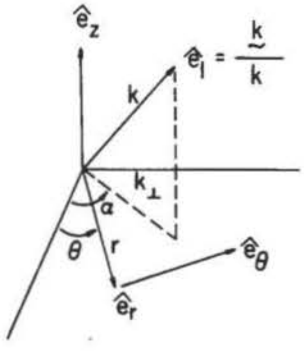

FIG. 2. **X** space and **k** space.

Fig. 2) defined by $\hat{e}_1$, $\hat{e}_2$, $\hat{e}_3$ where

$$\hat{e}_1 = \mathbf{k}/k, \quad \hat{e}_3 = (1/k_\perp)\mathbf{k}\times\hat{e}_z, \text{ and } \hat{e}_2 = \hat{e}_3\times\hat{e}_1.$$

In terms of these unit vectors,

$$\begin{aligned}\hat{e}_r &= \hat{e}_1(k_\perp/k)\cos(\alpha-\theta) + \hat{e}_2(is/kv_0)\cos(\alpha-\theta) \\ &\quad + \hat{e}_3\sin(\alpha-\theta), \\ \hat{e}_\theta &= \hat{e}_1(k_\perp/k)\sin(\alpha-\theta) + \hat{e}_2(is/kv_0)\sin(\alpha-\theta) \\ &\quad - \hat{e}_3\cos(\alpha-\theta), \\ \hat{e}_z &= -\hat{e}_1(is/kv_0) + \hat{e}_2(k_\perp/k).\end{aligned} \tag{5}$$

Transforming Eqs. (3) and (4) into the new frame, we then derive Ohm's law in **k** space. The result is

$$\delta\mathbf{J}(\mathbf{k}) = n_0 e[\delta v_i(\mathbf{k}) - \delta v_e(\mathbf{k})] = \boldsymbol{\sigma}\cdot\delta\mathbf{E}(\mathbf{k}), \tag{6}$$

where the conductivity tensor $\boldsymbol{\sigma}$ is given in Appendix A.

It is advantageous to use the Green's function method to treat the variable r, namely, we first obtain the responses of the plasma to a shell current of infinitesimal thickness expressed by

$$J_b(\mathbf{x},r') = (-n_b e/2\pi r)S(-Z)\delta(r-r')(r\omega\hat{e}_\theta + v_0\hat{e}_z), \tag{7}$$

where

$$S(x) = \begin{cases}1 & \text{for } x>0 \\ 0 & \text{for } x<0\end{cases}$$

is the step function, and $\delta(x)$ is the Dirac delta function, then integrate the results over r' over the actual beam thickness. Henceforth, we will denote the Green's functions by writing them explicitly as functions of r' as in Eq. (7).

Combining Ampere's, Faraday's, and Ohm's laws, we obtain the Green's function equation for the electric field in k space

$$\left(k^2 + \frac{s^2}{c^2} - \mathbf{kk} - \frac{4\pi s}{c^2}\boldsymbol{\sigma}\right)\cdot\delta\mathbf{E}(\mathbf{k},r') = \frac{4\pi s}{c^2}\mathbf{J}_b(\mathbf{k},r'), \tag{8}$$

where the shell current

$$\mathbf{J}_b(\mathbf{k},r') = \int \mathbf{J}_b(\mathbf{x},r')\exp(-i\mathbf{k}\cdot\mathbf{x})\,d^3x$$

$$= \frac{n_b e v_0}{k(s-\delta)}[-isJ_0(k_\perp r')\hat{e}_1 + k_\perp v_0 J_0(k_\perp r')\hat{e}_2 + ikr'\omega J_1(k_\perp r')\hat{e}_3]$$

serves as the source term, J_0 and J_1 are Bessel functions of order zero and one, respectively, and δ is an infinitesimally positive number.

With $\boldsymbol{\sigma}$ substituted for by its explicit expression, Eq. (8) becomes

$$\boldsymbol{\alpha}\cdot\delta\mathbf{E}(\mathbf{k},r') = k^2 s\Delta(s)\mathbf{J}_b(\mathbf{k},r'), \tag{9}$$

where

$$\Delta(s) = 4\pi(s-\nu_e)[(s-\nu_e)^2 + \Omega_e^2][(s-\nu_i)^2 + \Omega_i^2]$$

and $\boldsymbol{\alpha}$ is given in Appendix B.

Inverting the matrix $[\boldsymbol{\alpha}]$ yields the expression for the electric field

$$\delta\mathbf{E}(\mathbf{k},r') = \frac{k^2 s\Delta(s)}{D(k_\perp,s)}\boldsymbol{\kappa}\cdot\mathbf{J}_b(\mathbf{k},r'), \tag{10}$$

where

$$D(k_\perp,s) = \det|\boldsymbol{\alpha}|$$

and

$$[\boldsymbol{\kappa}] = \text{adjoint matrix of } [\boldsymbol{\alpha}].$$

We are now able to calculate the magnetic field through Faraday's law

$$\delta\mathbf{B}(\mathbf{k},r') = (ikc/s)\hat{e}_1\times\delta\mathbf{E}(\mathbf{k},r') \tag{11}$$

and the plasma current density through Ohm's law

$$\delta\mathbf{J}(\mathbf{k},r') = [k^2 s\Delta(s)/D(k_\perp,s)]\boldsymbol{\sigma}\cdot\boldsymbol{\kappa}\cdot\mathbf{J}_b(\mathbf{k},r'). \tag{12}$$

With the help of Eq. (5), we obtain $\delta\mathbf{J}$ in the cylindrical frame

$$\begin{aligned}\delta J_r(\mathbf{k},r') &= \delta J_1(\mathbf{k},r')(k_\perp/k)\cos(\alpha-\theta) \\ &\quad + \delta J_2(\mathbf{k},r')(is/kv_0)\cos(\alpha-\theta) \\ &\quad + \delta J_3(\mathbf{k},r')\sin(\alpha-\theta),\end{aligned}$$

$$\begin{aligned}\delta J_\theta(\mathbf{k},r') &= \delta J_1(\mathbf{k},r')(k_\perp/k)\sin(\alpha-\theta) \\ &\quad + \delta J_2(\mathbf{k},r')(is/kv_0)\sin(\alpha-\theta) \\ &\quad - \delta J_3(\mathbf{k},r')\cos(\alpha-\theta),\end{aligned}$$

$$\delta J_z(\mathbf{k},r') = -\delta J_1(\mathbf{k},r')(is/kv_0) + \delta J_2(\mathbf{k},r')(k_\perp/k),$$

and similar expressions for the electric and magnetic fields.

We now obtain the x space quantities by performing and inverse Fourier transform of their corresponding **k** space expressions. In doing so, we note that the α integrations are facilated by the standard integrals

$$\int_0^{2\pi} d\alpha \exp[ik_\perp 1 r\cos(\alpha-\theta)] \begin{Bmatrix} 1 \\ \cos(\alpha-\theta) \\ \sin(\alpha-\theta) \end{Bmatrix} = 2\pi \begin{Bmatrix} J_0(k_\perp r) \\ iJ_1(k_\perp) \\ 0 \end{Bmatrix}$$

thus

$$\begin{Bmatrix} \delta J_\theta(\mathbf{x},r') \\ \delta J_z(\mathbf{x},r') \\ \delta E_r(\mathbf{x},r') \\ \delta E_\theta(\mathbf{x},r') \\ \delta E_z(\mathbf{x},r') \end{Bmatrix} = \frac{in_b e}{(2\pi)^2}\int_0^\infty k_\perp dk_\perp \int_{-i\infty}^{i\infty} ds \frac{\Delta(s)\exp(sZ/v_0)}{D(k_\perp,s)} \begin{Bmatrix} W_\theta(k_\perp,s,r')J_1(k_\perp r) \\ W_z(k_\perp,s,r')J_0(k_\perp r) \\ X_r(k_\perp,s,r')J_1(k_\perp r) \\ X_\theta(k_\perp,s,r')J_1(k_\perp r) \\ X_z(k_\perp,s,r')J_0(k_\perp r) \end{Bmatrix}, \tag{13a}$$

$$\delta B_r(\mathbf{x},r') = -(c/v_0)\delta E_\theta(\mathbf{x},r'), \tag{13b}$$

$$\delta B_z(\mathbf{x},r') = \frac{in_b e}{(2\pi)^2}\int_0^\infty k_\perp dk_\perp \int_{-i\infty}^{i\infty} \frac{\Delta(s)\exp(sZ/v_0)}{(s-\delta)D(k_\perp,s)} \times Y_z(k_\perp,s,r')J_0(k_\perp r), \tag{13c}$$

where the functions W_θ through Y_z are given in Appendix C. All of them are of the form of a function of $k_\perp$ and s times a Bessel function of argument $k_\perp r'$.

Thus far, the solutions are obtained exactly but in an integral form are not readily subject to analytic analysis. In the next section, we shall seek analytic solutions for restricted but realistic parameter regimes.

III. NONOSCILLATORY SOLUTIONS

The s integrations of Eqs. (13) will now be carried out by the method of contour integration. The essential use we are going to make of this method is that by locating only a few pertinent poles, we can extract from Eqs. (13) all the desired information despite the complexity of their forms.

We intend to reduce the integrands to a solvable form by order of magnitude considerations of the parameters therein, such as ν, ω_p, and Ω, etc. To this end, it is necessary to consider the following:

i. Our primary interest lies in the case in which a substantial drift angular counter current will be induced by the beam because, firstly, the radial electric field associated with this current can lead to significant heating of ions (treated in detail later). Secondly, with our rigid beam assumption and linearization of the equations of motion, we have practically neglected the effects of the beam self-magnetic field on the motion of the beam or plasma particles. This would be self-consistent if the beam is fully current neutralized.

It was argued in Sec. I that the formation of a drift angular counter current is highly dependent on the collisional effects. From the same argument, we infer a condition under which the existence of such a current is possible, namely,

$$\Omega_e \gg \nu_e, \quad \Omega_i \ll \nu_i. \tag{14}$$

Physically, the condition implies that the ions are unmagnetized.

As expected, under this condition, the ratio of the Hall component of the ion mobility tensor to that of the electrons (see Appendix D) is much less than one

$$\frac{\mu_{ir\theta}}{\mu_{er\theta}} = \frac{m\Omega_i(\Omega_e^2+\nu_e^2)}{M\Omega_e(\Omega_i^2+\nu_i^2)} \approx \frac{\Omega_i^2}{\nu_i^2} \ll 1.$$

Therefore, a radial electric field will drive a net electron drift current δJ_θ in the plasma.

ii. In distinction to other phenomena involved, the counter plasma currents and related quantities are nonoscillatory in nature, and have a decay time longer than ν_e^{-1} because of the inductive effect. These two properties enable us to narrow our effort to the determination of poles (denoted by subscript j) satisfying $0 < s_j < \nu_e$. This way we can leave the oscillatory poles alone, which, in general, have imaginary parts much greater than ν_e.

iii. All the integrands in Eqs. (13) are proportional to the product of $k_\perp$ and two Bessel functions (of order 0 or 1) with argument $\approx k_\perp a$, where a is the average radius of the beam. A close look at their behavior shows that the dominant contribution to the integrals would be in the neighborhood of $k_\perp \approx a^{-1}$, provided the other factors of the integrands are relatively smooth over this range of $k_\perp$. When the poles are determined, it can be shown *a posteriori* that this is indeed the case. Since $a \le c/\omega \le c/\Omega_e$, we thus have $k_\perp c \ge \Omega_e$ for the dominant range of $k_\perp$.

iv. Finally, we add the assumption $\omega_p \gg \nu_e$, where

$$\omega_p^2 = 4\pi n_0 e^2/m.$$

This assumption merely states that the collective plasma behavior is not critically damped.

To sum up, we have grouped all the parameters according to their order of magnitude as follows:

$$\omega_p,\ \Omega_e,\ k_\perp v_0,\ k_\perp c \gg \nu_e,\ \nu_i,\ s_j\,, \quad \nu_i \gg \Omega_i. \tag{15}$$

It should be noted that, in reaching these relations, we have made only one special assumption, the inequalities in (14).

With the help of (15), we can now expand the integrands and thereby neglect all but the lowest order terms. The lengthy expansions will not be given here. However, we point out one essential detail about the way the approximation was carried out. Since no assumptions were made about the relationship of parameters belonging to the same group, we have seen to it that the terms to be dropped were unambiguously of next order compared to any of the remaining ones. For example, when two terms, such as $\Omega_e \Omega_i$ and $\nu_e \nu_i$, $k_\perp c$ and ω_p, etc., were not comparable according to (15), they were both retained.

Since $k_\perp c$ belongs to the *largest* parameter group for reasons given earlier, the fact that $k_\perp$ is a variable and $k_\perp c$ may take smaller values will apparently not nullify our results.

With all higher order terms neglected, we are then able to determine the poles, carry out the contour integration over s (see Fig. 3), and obtain the solutions regarding current neutralization. It should be noted that the solutions so obtained are only the nonoscillatory part of the total solutions, although, for simplicity, we shall not mark them explicitly.

$$\delta J_\theta(\mathbf{x},r') = \frac{n_b e}{2\pi} S(-Z) \int_0^\infty dk_\perp J_1(k_\perp r)\left[\frac{k_\perp r'\omega J_1(k_\perp r')}{1+k_\perp^2\lambda^2}\sum_{j=2}^{3}\frac{(s_j - s_j)(s_j-\nu_i)}{(s_j-s_2)(s_j-s_3)}\exp(s_j Z/v_0) - \frac{k_\perp^4\lambda^4\Omega_e J_0(k_\perp r)}{(1+k_\perp^2\lambda^2)^2}\sum_{j=1}^{3}\frac{(s_j-s_j)(s_j-\nu_e)(s_j-\nu_i)}{(s_j-s_1)(s_j-s_2)(s_j-s_3)}\exp(s_j Z/v_0)\right], \quad (16a)$$

$$\delta J_z(\mathbf{x},r') = \frac{n_b e v_0}{2\pi} S(-Z)\int_0^\infty dk_\perp J_0(k_\perp \cap r) \left\{\frac{k_\perp J_0(k_\perp r')}{1+k_\perp^2\lambda^2}\exp\left(\frac{k_\perp^2\lambda^2\nu_e Z}{(1+k_\perp^2\lambda^2)v_0}\right) + \frac{k_\perp^2\lambda^2\Omega_e[r'\omega J_1(k_\perp r') - k_\perp\lambda^2\Omega_e J_0(k_\perp r)]}{(1+k_\perp^2\lambda^2)^2 v_0^2}\sum_{j=1}^{3}\frac{(s_j-s_j)s_j(s_j-\nu_i)}{(s_j-s_1)(s_j-s_2)(s-s_3)}\exp(s_j Z/v_0)\right\}, \quad (16b)$$

$$\delta E_r(\mathbf{x},r') = \frac{4\pi\Omega_e}{\omega_p^2}\delta J_\theta(\mathbf{x},r'), \quad (16c)$$

$$\delta E_z(\mathbf{x},r') = \frac{2n_b e v_0}{\omega_p^2} S(-Z)\int_0^\infty dk_\perp J_0(k_\perp r)\left\{\frac{k_\perp \nu_e J_0(k_\perp r')}{(1+k_\perp^2\lambda^2)^2}\exp\left(\frac{k_\perp^2\lambda^2\nu_e Z}{(1+k_\perp^2\lambda^2)v_0}\right) - \frac{k_\perp^2\lambda^2\Omega_e[r'\omega J_1(k_\perp r') - k_\perp\lambda^2\Omega_e J_0(k_\perp r')]}{(1+k_\perp^2\lambda^2)^2 v_0^2}\sum_{j=1}^{3}\frac{(s_j-s_j)s_j(s_j-\nu_i)s_j-\nu_e)}{(s_j-s_1)(s_j-s_2)(s_j-s_3)} \times \exp(s_j Z/v_0)\right\}, \quad (16d)$$

$$\begin{aligned}\delta E_\theta(\mathbf{x},r') &= -(v_0/c)\delta B_r(\mathbf{x},r') \\ &= \frac{-2n_b e}{\omega_p^2} S(-Z)\int_0^\infty dk_\perp J_1(k_\perp r)\left\{\frac{k_\perp r'\omega J_1(k_\perp r')}{1+k_\perp^2\lambda^2} \times \sum_{j=2}^{3}\frac{(s_j-s_j)[(s_j-\nu_e)(s_j-\nu_i)+\Omega_i\Omega_e]}{(s_j-s_2)(s_j-s_3)}\exp(s_j Z/v_0) + \frac{k_\perp^2\lambda^2\Omega_e J_0(k_\perp r)}{(1+k_\perp^2\lambda^2)^2}\sum_{j=1}^{3}\frac{(s_j-s_j)s_j(s_j-\nu_i)(s_j-\nu_e)}{(s_j-s_1)(s_j-s_2)(s_j-s_3)}\exp(s_j Z/v_0)\right\},\end{aligned} \quad (16e)$$

$$\delta B_z(\mathbf{x},r') = \frac{-2n_b e}{c} S(-Z)\int_0^\infty dk_\perp J_0(k_\perp r) \left\{r'\omega J_1(k_\perp r')\left[1 + \frac{k_\perp^2\lambda^2}{1+k_\perp^2\lambda^2}\sum_{j=2}^{3}\frac{(s_j-s_j)[(s_j-\nu_e)(s_j-\nu_i)+\Omega_e\Omega_i]}{s_j(s_j-s_2)(s_j-s_3)}\exp(s_j Z/v_0)\right] + \frac{k_\perp^3\lambda^4\Omega_e J_0(k_\perp r')}{(1+k_\perp^2\lambda^2)^2}\sum_{j=1}^{3}\frac{(s_j-s_j)(s_j-\nu_e)(s_j-\nu_i)}{(s_j-s_1)(s_j-s_2)(s_j-s_3)}\exp(s_j Z/v_0)\right\}, \quad (16f)$$

where $\lambda = c/\omega_p$ is the plasma skin depth, and

$$s_1 = k_\perp^2\lambda^2\nu_e/(1+k_\perp^2\lambda^2), \quad s_{2,3} = \frac{(1+k_\perp^2\lambda^2)\nu_i + k_\perp^2\lambda^2\nu_e \pm \{[(1+k_\perp^2\lambda^2)\nu_i - k_\perp^2\lambda^2\nu_e]^2 - 4k_\perp^2\lambda^2(1+k_\perp^2\lambda^2)\Omega_e\Omega_i\}^{1/2}}{2(1+k_\perp^2\lambda^2)}.$$

One has to turn to numerical methods to solve Eqs. (16) in their present forms. However, these integrals can be carried out approximately for realistic parameter regimes. A generally known condition for substantial current neutralization is $a \gg \lambda$. This condition is easily satisfied for our problem, since for a hollow beam of reasonable physical size, we have $a \geq 3$ cm, and by assumption, $n_0 \geq 10^{12}/\text{cm}^3$ or $\lambda \leq 0.5$ cm. We recall that the dominant value of $k_\perp$ centers at $k_\perp \approx a^{-1}$, thus for all practical purposes, $k_\perp^2\lambda^2 \approx \lambda^2/a^2 \ll 1$. As a result, the last term in each of the integrands in Eqs. (16) only gives contributions of order (λ^2/a^2) or higher compared to the other terms. To a first approximation, we shall neglect those higher-order terms.

In order to simplify the expressions for s_2 and s_3, we assume

$$\nu_i^2/\Omega_e\Omega_i \gg 4(\lambda^2/a^2) \tag{17}$$

which should generally hold in the light of the relation $a \gg \lambda$.

With this assumption, we can expand the square roots in s_2 and s_3 to obtain

$$\begin{aligned} s_2 &\approx \left(1 - \frac{k_\perp^2\lambda^2\Omega_e\Omega_i}{(1+k_\perp^2\lambda^2)\nu_i^2}\right)\nu_i \\ s_3 &\approx \frac{k_\perp^2\lambda^2\nu_\perp}{1+k_\perp^2\lambda^2} \end{aligned} \tag{18}$$

where $\nu_\perp = \nu_e(1+\Omega_e\Omega_i/\nu_e\nu_i)$ is the effective collision frequency in the perpendicular direction.

Note that all the poles (s_1 through s_3) are consistent with the condition $0 < s_j < \nu_e$ set forth before.

Substituting Eq. (18) into Eq. (16a) gives

$$\begin{aligned} \delta J_\theta(\mathbf{x}, r') = {} & \frac{n_b e r'\omega}{2\pi} S(-Z)\int_0^\infty k_\perp dk_\perp J_1(k_\perp r)J_1(k_\perp r') \\ & \times\left\{\frac{1}{1+k_\perp^2\lambda^2}\exp\left(-\frac{k_\perp^2\lambda^2\nu_\perp Z}{(1+k_\perp^2\lambda^2)v_0}\right)\right. \\ & \left. - \frac{k_\perp^2\lambda^2\Omega_e\Omega_i}{(1+k_\perp^2\lambda^2)^2\nu_i^2}\exp\left[\left(1-\frac{k_\perp^2\lambda^2\Omega_e\Omega_i}{(1+k_\perp^2\lambda^2)\nu_i^2}\right)\frac{\nu_i Z}{v_0}\right]\right\}. \end{aligned} \tag{19}$$

The second term, which has a decay time $\approx \nu_i^{-1}$, is due to the ion relaxation effect. We shall neglect this term because its magnitude is of order (λ^2/a^2) compared with the first term by virtue of (17).

Using standard integral tables,[25] from Eq. (19) we obtain

$$\delta J_\theta(\mathbf{x}, r') \approx \frac{n_b e\omega}{2\pi\lambda^2} S(-Z)\exp\left(\frac{Z}{l_\perp}\right) r' I_1\left(\frac{r_<}{\lambda}\right)K_1\left(\frac{r_>}{\lambda}\right), \tag{20a}$$

where

$$l_\perp = \frac{(a^2+\lambda^2)v_0}{\lambda^2\nu_\perp};$$

$r_>$ and $r_<$ are the larger and smaller of r and r', respectively, I_1 and K_1 are modified Bessel functions, and as an approximation, we have replaced $k_\perp$ in the exponential of Eq. (19) by its average value a^{-1}.

Owing to an attached condition set forth earlier for this last approximation, Eq. (20a) is valid for $|Z/l_\perp| \leq 1$ only. For $|Z/l_\perp| > 1$, the exponential factor will change the behavior of the integrand such that its dominant value is no longer in the neighborhood of $k_\perp \approx a^{-1}$. In other words, Eq. (20a) (and equations derived later in the same manner) is valid until δJ_θ decays to about half of its full value. It will be apparent later that this is in fact the same limitation resulting from our constant velocity beam model, because long before the plasma currents decay away, the beam axial velocity will be so reduced that the model breaks down. Our main concern, however, will be the front portion of the beam where all results are valid.

Similarly, we obtain from the rest of Eqs. (16)

$$\delta J_z(\mathbf{x}, r') \approx \frac{n_b e v_0}{2\pi\lambda^2} S(-Z)\exp\left(\frac{Z}{l_\parallel}\right) I_0\left(\frac{r_<}{\lambda}\right)K_0\left(\frac{r}{\lambda}\right), \tag{20b}$$

$$\delta E_r(\mathbf{x}, r') = (4\pi\Omega_e/\omega_p^2)\delta J_\theta(\mathbf{x}, r'), \tag{20c}$$

$$\delta E_z(\mathbf{x}, r') \approx \frac{2n_b e v_0\nu_e a^2}{c^2(a^2+\lambda^2)} S(-Z)\exp\left(\frac{Z}{l_\parallel}\right) I_0\left(\frac{r_>}{\lambda}\right)K_0\left(\frac{r_>}{\lambda}\right), \tag{20d}$$

$$\begin{aligned} \delta E_\theta(\mathbf{x}, r') &= -(v_0/c)\delta B_r(\mathbf{x}, r') \\ &\approx \frac{2n_b e\omega a^2\nu_\perp}{c^2(a^2+\lambda^2)} S(-Z)\exp\left(\frac{Z}{l_\perp}\right) r' I_1\left(\frac{r_<}{\lambda}\right)K_1\left(\frac{r_>}{\lambda}\right), \end{aligned} \tag{20e}$$

$$\delta B_z(\mathbf{x}, r') \approx \frac{2n_b e\omega}{c} S(-Z) \begin{cases} -1 + \exp\left(\dfrac{Z}{l_\perp}\right)\left[1 - \dfrac{r'}{\lambda} I_0\left(\dfrac{r}{\lambda}\right)K_1\left(\dfrac{r'}{\lambda}\right)\right] & \text{for } r < r' \\ \exp\left(\dfrac{Z}{l_\perp}\right)\dfrac{r'}{\lambda} I_1\left(\dfrac{r'}{\lambda}\right)K_0\left(\dfrac{r}{\lambda}\right) & \text{for } r > r', \end{cases} \tag{20f}$$

where

$$l_\parallel = (a^2+\lambda^2)v_0/\lambda^2\nu_e.$$

In the remaining part of the paper, Eqs. (20) will be used to look into the physical aspects of the problem.

IV. CURRENT NEUTRALIZATION

The beam-induced plasma current δJ_θ may be calculated from its Green's function by an integration over the beam cross section. Assuming the hollow beam has inner radius a_1 and outer radius a_2, we then obtain from Eq. (20a)

$$\delta J_\theta(\mathbf{x}) = \int_{a_1}^{a_2} \delta J_\theta(\mathbf{x}, r') 2\pi r' \, dr'$$

$$= n_b e r \omega \, S(-Z) \exp\left(\frac{Z}{l_\perp}\right)$$

$$\left[1 - \frac{a_1^2}{r\lambda} I_2\left(\frac{a_1}{\lambda}\right) K_1\left(\frac{r}{\lambda}\right) - \frac{a_2^2}{r\lambda} I_1\left(\frac{r}{\lambda}\right) K_2\left(\frac{a_2}{\lambda}\right)\right],$$

$$\text{for } a_1 < r < a_2, \tag{21}$$

where the integral was solved exactly by employing the following relations:

$$\int x^{n+1} \begin{Bmatrix} I_n(x) \\ K_n(x) \end{Bmatrix} dx = x^{n+1} \begin{Bmatrix} I_{n+1}(x) \\ -K_{n+1}(x) \end{Bmatrix}$$

$$I_n(x) K_{n+1}(x) + I_{n+1}(x) K_n(x) = 1/x.$$

Since r/λ, a_1/λ, $a_2/\lambda \gg 1$, the asymptotic expressions for modified Bessel functions may be used:

$$\begin{aligned} I_n(x) &\sim (2\pi x)^{-1/2} e^x \\ K_n(x) &\sim (\pi/2x)^{1/2} e^{-x} \end{aligned} \tag{22}$$

thus

$$\delta J_\theta(Z < 0) \approx n_b e r \omega \exp\left(\frac{Z}{l_\perp}\right)$$

$$\left[1 - \frac{1}{2}\left(\frac{a_1}{r}\right)^{3/2} \exp\left(\frac{a_1 - r}{\lambda}\right) - \frac{1}{2}\left(\frac{a_2}{r}\right)^{3/2} \exp\left(\frac{r - a_2}{\lambda}\right)\right], \text{ for } a_1 < r < a_2,$$

where, as we shall do henceforth, the factor $S(-Z)$ has been replaced by "$Z < 0$" in the parenthesis.

Assuming $a_2 - a_1 \gg \lambda$, we find that the angular beam current is almost totally neutralized by δJ_θ except within the skin depth λ from both boundary surfaces.

Outside the beam, we obtain

$$\delta J_\theta(Z < 0) = \frac{n_b e \omega}{\lambda} \exp\left(\frac{Z}{l_\perp}\right)$$

$$\begin{cases} K_1\left(\frac{r}{\lambda}\right)\left[a_2^2 I_2\left(\frac{a_2}{\lambda}\right) - a_1^2 I_2\left(\frac{a_1}{\lambda}\right)\right], & r > a_2 \\ I_1\left(\frac{r}{\lambda}\right)\left[a_1^2 K_2\left(\frac{a_1}{\lambda}\right) - a_2^2 K_2\left(\frac{a_2}{\lambda}\right)\right], & r < a_1. \end{cases}$$

By use of Eqs. (22), these currents can be shown to drop sharply and exponentially away from the beam boundaries with a decay distance λ.

For the radial electric field, Eq. (16c) yields

$$\delta E_r(Z < 0) = (4\pi \Omega_e/\omega_p^2) \delta J_\theta(Z < 0) \tag{23}$$

which then gives

$$\delta J_\theta(Z < 0) = (n_0 e c/B_0) \delta E_r(Z < 0).$$

Thus δJ_θ is explicitly shown to be an $E \times B$ drift current (Fig. 4). [Drift type counter currents were also found by Lee and Sudan using a different geometry.[5]]

In contrast to the axial counter current which is always driven by an axial electric field, the angular counter can be driven by either a radial electric field through $\delta J_\theta = -n_0 e \mu_{e\theta r} \delta E_r$, or by an azimuthal electric field through $\delta J_\theta = -n_0 e \mu_{e\theta\theta} \delta E_\theta$, where $\mu_{e\theta r}$ and $\mu_{e\theta\theta}$ are, respectively, the Hall and diagonal component of the electron mobility tensor as defined in Appendix D. In our case, $\Omega_e \gg \nu_e$ or $\mu_{e\theta r} \gg \mu_{e\theta\theta}$, it is thus clear that the former mechanism has taken place because it requires a smaller driving electric field.

δE_r is produced by a net space charge ρ given by Poisson's equation. For $a_1 < r < a_2$,

$$\rho(Z < 0) = \rho_b + \delta\rho(Z < 0)$$

$$= \frac{\omega \Omega_e}{\omega_p^2} |\rho_b| \exp\left(\frac{Z}{l_\perp}\right) \times \left[2 + \left(\frac{a_1}{\lambda}\right)^2 I_2\left(\frac{a_1}{\lambda}\right) K_0\left(\frac{r}{\lambda}\right) - \left(\frac{a_2}{\lambda}\right)^2 I_0\left(\frac{r}{\lambda}\right)^2 K_2\left(\frac{a_2}{\lambda}\right)\right], \tag{24}$$

where $\rho_b = -n_b e$ is the beam charge density.

Since $\Omega_e \approx \gamma\omega$ and $a\omega \approx c$, Ω_e is related to a by

$$\Omega_e \approx \gamma c/a. \tag{25}$$

Eliminating ω and Ω_e in Eq. (24) by means of Eq. (25) and neglecting the modified Bessel functions, we obtain

$$\rho(Z < 0) \approx 2\gamma(\lambda^2/a^2)|\rho_b| \ll |\rho_b|, \qquad a_1 < r < a_2.$$

Thus, as a result of its rotation, the beam is actually slightly overneutralized.

The calculation for other quantities from their Green's functions is the same as for δJ_θ. From Eq. (20b), we obtain

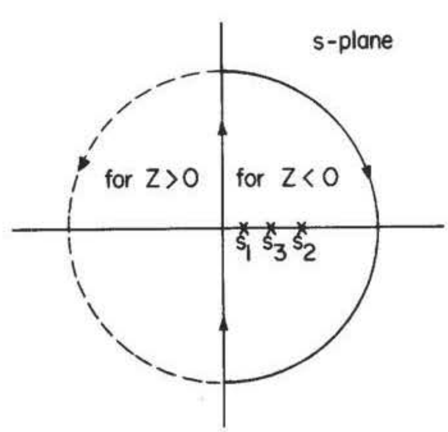

FIG. 3. Contours for s integration.

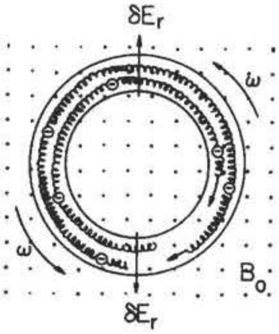

FIG. 4. $\delta E_r \times B_0$ drift motion of plasma electrons.

$$\delta J_z(Z<0) = n_b e v_0 \exp\left(\frac{Z}{l_\parallel}\right)$$
$$\begin{cases} \frac{1}{\lambda}\left[a_2 I_1\left(\frac{a_2}{\lambda}\right)K_0\left(\frac{r}{\lambda}\right) - a_1 I_1\left(\frac{a_1}{\lambda}\right)K_0\left(\frac{r}{\lambda}\right)\right], & r>a_2 \\ 1-\frac{1}{2}\left(\frac{a_1}{r}\right)^{1/2}\exp\left(\frac{a_1-r}{\lambda}\right) - \frac{1}{2}\left(\frac{a_2}{r}\right)^{1/2}\exp\left(\frac{r-a_2}{\lambda}\right), & \\ \quad a_1<r<a_2 & \\ \frac{1}{\lambda}\left[a_1 I_0\left(\frac{r}{\lambda}\right)K_1\left(\frac{a_1}{\lambda}\right) - a_2 I_0\left(\frac{r}{\lambda}\right)K_1\left(\frac{a_2}{\lambda}\right)\right], & r<a_1. \end{cases} \tag{26}$$

The axial beam current is also shown to be neutralized as one would expect from earlier works on nonrotational beams. In fact, the rotational motion of the beam only affects the axial current neutralization through second-order terms which are shown in Eq. (16b), but later neglected to a first approximation.

The two decay distances:

$$l_\perp = (a^2+\lambda^2)v_0/\lambda^2\nu_\perp = (a^2+\lambda^2)v_0/\lambda^2(1+\Omega_e\Omega_i/\nu_e\nu_i)\nu_e, \quad \text{for } \delta J_\theta$$

and

$$l_\parallel = (a^2+\lambda^2)v_0/\lambda^2\nu_e, \quad \text{for } \delta J_z$$

can be interpreted as follows. The first term in the denominator of $l_\perp$ apparently originates from the collisional damping of electron current, as does the whole expreesion for $l_\parallel$. The second term in the denominator of $l_\perp$ is due to a different decay mechanism special to the angular counter current. In Eq. (24) we have shown the existence of a net space charge necessary to sustain δJ_θ. This space charge, however, is subject to neutralization by radial flow of the plasma particles. Because of their small collision to cyclotron frequency ratio, the plasma electrons are mainly drifting angularly rather than flowing radially under the influence of δE_r. As a result, their charge neutralizing effect, expressed by the first term in the denominator of $l_\perp$, is limited although by no means negligible for the time scale under consideration. On the other hand, the ions, little affected by the magnetic field, are obstructed only by collisions. Their charge neutralizing effect may therefore be much greater than that of the electrons despite their larger inertia. To illustrate this point quantitatively, let us compare the diagonal components of the mobility tensor for the two species (see Appendix D).

$$\frac{\mu_{irr}}{\mu_{err}} = \frac{m\nu_i(\nu_e^2+\Omega_i^2)}{M\nu_e(\nu_i^2+\Omega_i^2)} \approx \frac{\Omega_e\Omega_i}{\nu_e\nu_i}.$$

This is precisely the ratio of the two terms in the denominator of $l_\perp$. So, clearly, it is the ion radial flow that accounts for the second term. We also note that the magnitude of this term could considerably exceed that of the first term within our assumptions.

The gradual space charge neutralization caused by the radial flow of the plasma particles will be accompanied by the slowing down of the electron velocity, hence the decay of δJ_θ.

The factor $(a^2+\lambda^2)/\lambda^2$ in $l_\perp$ and $l_\parallel$ is attributable to the strong inductive property of the system, namely, whenever a current changes its magnitude, a proper electric field will be induced to accelerate the plasma particles in such a way as to counter the change. For our present case, Eqs. (20b,d) and (20a,e) give

$$\begin{bmatrix}\delta E_z\ (Z<0)\\ \delta E_\theta\ (Z<0)\end{bmatrix} = \frac{4\pi a^2 v_0}{c^2}\frac{\partial}{\partial Z}\begin{bmatrix}\delta J_z\ (Z<0)\\ \delta J_\theta\ (Z<0)\end{bmatrix}. \tag{27}$$

Here, δE_z and δE_θ are explicitly shown to be proportional to the decay of δJ_z and δJ_θ, respectively. It is these inductive rate fields that give rise to the lengthening factor $(a^2+\lambda^2)/\lambda^2$ in $l_\perp$ and $l_\parallel$.

In addition to δE_θ, the decay of δJ_θ also induces a radial magnetic field δB_r. From Eqs. (20a,e),

$$\delta B_r(Z<0) = (-4\pi a^2/c)(\partial/\partial z)\delta J_\theta(Z<0). \tag{28}$$

It will be shown, in the next two sections, that the perturbed fields in Eqs. (23), (27), and (28) provide the essential mechanisms for beam–plasma interactions.

From Eq. (20f), we obtain

$$\delta B_z(Z<0) = \omega_{pb}^2 B_0/\gamma c^2$$
$$\times\begin{cases} \exp\left(\frac{Z}{l_\perp}\right)K_0\left(\frac{r}{\lambda}\right)\left[a_2^2 I_2\left(\frac{a_2}{\lambda}\right) - a_1^2 I_2\left(\frac{a_1}{\lambda}\right)\right], \text{ for } r>a_2 \\ -\frac{1}{2}(a_2^2-r^2)\left[1-\exp\left(\frac{Z}{l_\perp}\right)\right] \\ \quad + \exp\left(\frac{Z}{l_\perp}\right)I_0\left(\frac{r}{\lambda}\right)\left[a_2^2K_2\left(\frac{a_2}{\lambda}\right) - r^2K_2\left(\frac{r}{\lambda}\right)\right] \\ +\exp\left(\frac{Z}{l_\perp}\right)K_0\left(\frac{r}{\lambda}\right)\left[r^2 I_2\left(\frac{r}{\lambda}\right) - a_1^2 I_2\left(\frac{a_1}{\lambda}\right)\right], \\ \quad \text{for } a_1<r<a_2 \\ -\frac{1}{2}(a_2^2-a_1^2)\left[1-\exp\left(\frac{Z}{l_\perp}\right)\right] \\ \quad + \exp\left(\frac{Z}{l_\perp}\right. \quad I_0\left(\frac{r}{\lambda}\right)\left[a_2^2K_2\left(\frac{a_2}{\lambda}\right) - a_1^2K_2\left(\frac{a_1}{\lambda}\right)\right], \\ \quad \text{for } r<a_1, \end{cases}$$

where

$$\omega_{pb}^2 = 4\pi n_b e^2/m.$$

The total axial magnetic field is

$$B_t(Z<0) = B_0 + \delta B_z(Z<0)$$

$$\approx \begin{cases} B_0\left\{1 - \frac{\omega_{pb}^2}{2\gamma c^2}(a_2^2 - r^2)[1 - \exp(Z/l_\perp)]\right\} a_1 < r < a_2 \\ B_0\left\{1 - \frac{\omega_{pb}^2}{2\gamma c^2}(a_2^2 - a_1^2)[1 - \exp(Z/l_\perp)]\right\} r < a_1 . \end{cases} \quad (29)$$

As shown in Eq. (29), B_t gradually decays from B_0 to zero and possibly to negative values as Z becomes more and more negative. We obtain therefrom the condition for axial magnetic field reversal

$$\omega_{pb}^2(a_2^2 - a_1^2)/2\gamma c^2 \geq 1.$$

If $n_b \geq 10^{11}/\mathrm{cm}^3$, this condition can easily be satisfied.

V. RETARDING FORCES ON THE BEAM–BEAM TRAPPING

Now that the beam-induced currents and fields are known, we shall look into the effects of the induced fields on the beam itself, and show

i. that the beam electrons feel no net angular force, hence their angular momentum remains constant, and

ii. that the decay of δJ_z and δJ_θ each results in an axial retarding force on the beam.

The force on one beam electron due to the beam-induced electromagnetic fields is

$$\mathbf{F} = -e(\delta\mathbf{E} + c^{-1}\mathbf{v}_b \times \delta\mathbf{B}), \quad (30)$$

where

$$\mathbf{v}_b = r\omega\, \mathbf{e}_\theta + v_0 \mathbf{e}_z .$$

To prove (i), we simply take the θ component of Eq. (30) and recall Eq. (13b), thus

$$F_0 = -e_1[\delta E_\theta + (v_0/c)\delta B_r] = 0.$$

The result is obvious in the beam frame in which the beam electron has only an angular velocity, hence feels no angular magnetic force. The angular electrostatic force in this frame also vanishes since the magnetic flux through any beam cross section is a constant, and no δE_θ will be induced.

With δE_z and δB_r calculated from Eqs. (23) and (28), respectively, Eq. (30) then yields the explicit expression for F_z.

$$F_z = F_{z\parallel} + F_{z\perp}, \quad (31a)$$

where

$$F_{z\parallel} = -e\delta E_z = \frac{-n_b v_0 m v_z a^2}{n_0(a^2 + \lambda^2)} \exp\left(\frac{Z}{l_\parallel}\right) \left[1 - \frac{a_1}{\lambda} I_1\left(\frac{a_1}{\lambda}\right) K_0\left(\frac{r}{\lambda}\right) - \frac{a_2}{\lambda} I_0\left(\frac{r}{\lambda}\right) K_1\left(\frac{a_2}{\lambda}\right)\right] \quad (31b)$$

$$F_{z\perp} = -(e/c) r\omega\delta B_r = \frac{-n_b r^2 \omega^2\, m v_\perp a^2}{n_0 v_0(a^2 + \lambda^2)} \exp\left(\frac{Z}{l_\perp}\right) \times\left[1 - \frac{a_1^2}{r\lambda} I_2\left(\frac{a_1}{\lambda}\right) K_1\left(\frac{r}{\lambda}\right) - \frac{a_2^2}{r\lambda} I_1\left(\frac{r}{\lambda}\right) K_2\left(\frac{a_2}{\lambda}\right)\right] \quad (31c)$$

and the symbols "$\parallel$" and "$\perp$" have been used to distinguish quantities associated with δJ_z and δJ_θ, respectively.

As shown in Eq. (27), when δJ_z decays, δE_z will be induced to inhibit the decay. For the oppositely moving beam electrons, however, δE_z causes the retarding electric force $F_{z\parallel}$ as shown in Eq. (31b).

$F_{z\perp}$ is a magnetic force due to δB_r. That the decay of δJ_θ would generate δB_r is not as apparent as that it would generate δE_θ. It can be conveniently viewed the following way. Near the beam front where the current is almost fully neutralized, the magnetic field is essentially the applied field $B_0\hat{e}_z$. However, the spatial decay of δJ_θ leads to the gradual emergence of $J_{b\theta}$ away from the beam front. Because of its diamagnetic nature, this net unneutralized beam angular current has the effect of pushing the originally axial magnetic field lines out of the beam and thereby gives them a radial component (see Fig. 5).

Both $F_{z\parallel}$ and $F_{z\perp}$ point to the opposite direction of beam axial velocity, hence statement (ii) is verified.

The retarding force F_z has some favorable properties for trapping of electron beam between magnetic mirrors. For example, it is produced locally by the beam itself, thus free from the shielding effect of the plasma, a problem often arising when the retarding fields originate externally. For the usual experimental parameters, F_z can reach a magnitude capable of slowing down the beam considerably in less than a meter. Furthermore, the work done by F_z, instead of being dissipated externally as in the case of resistive ring trapping, is converted into the plasma internal energy. In the next section we shall show that this last advantage proves to be a significant heating mechanism for the plasma.

As a numerical example, we apply the results to the Cornell astron experiment.[19] At injection into a magnetic mirror, a relativistic electron beam ($\gamma = 2$) of 60-nsec duration is made to assume a helical orbit by an applied magnetic field (200 G). The pitch distance (6 cm) is only slightly larger than the beam diameter, therefore, the over-all beam shape and its motion roughly fit our hollow rotational beam model.

Granted full counter currents are induced, their retarding effect on the beam can be conveniently measured by a parameter f defined as the fractional beam axial energy loss per unit length. The average axial energy per beam electron is $(\gamma - \gamma_\perp)mc^2$, where

$$\gamma = (1/mc)\sqrt{m^2c^2 + p_{b\theta}^2 + p_{bz}^2}, \quad (32a)$$

and

$$\gamma_\perp = (1/mc)\sqrt{m^2c^2 + p_{b\theta}^2}. \quad (32b)$$

Thus,

$$f = F_z/(\gamma - \gamma_\perp)mc^2. \tag{33}$$

From Eqs. (31) pnd (33), we obtain

$$f = \frac{n_b v_0 a^2}{(\gamma - \gamma_\perp) n_0 c^2 (a^2 + \lambda^2)} \left[\nu_e \exp\left(\frac{Z}{l_\parallel}\right) + \frac{r^2\omega^2}{v_0^2} \nu_\perp \exp\left(\frac{Z}{l_\perp}\right) \right], \tag{34}$$

where, for clarity, we have neglected the skin depth effects represented by the modified Bessel function terms.

The known parameters are: $a \approx 9$ cm, $v_0 \approx 3 \times 10^9$ cm/sec, $\Omega_e \approx \gamma\omega \approx 3 \times 10^9$ rad/sec, $\Omega_i \approx 10^5$ rad/sec (note $a\omega \gg v_0$). Thus, on the right-hand side of Eq. (34), the first term, which originates from the δJ_z decay, is negligible compared with the second term, which originates from the δJ_θ decay.

The beam and plasma densities are approximately:

$$n_b \approx 10^{11}/\text{cm}^3,\ n_0 \approx 5 \times 10^{12}/(cm)^3,$$

so $\omega_p \approx 1.4 \times 10^{11}$ rad/sec, $\lambda \approx 0.23$ cm, $l_\perp \approx 480$ m, and $\exp(Z/l_\perp) \approx 1$. Accurate values of ν_e and ν_i are not available for lack of knowledge of plasma temperature. Let us for the moment assume $\nu_e \approx 10^8$/sec and $\nu_i \approx 5 \times 10^6$/sec so that the condition in Eq. (14) is satisfied and Eq. (34) is applicable. Substituting these values into Eq. (34) gives $f \approx 0.01$/cm.

As this example illustrates, in a distance of 50 cm, about half of the beam axial energy will be dissipated away by F_z.

A comment is in order here. Equation (34) is based on the assumption of constant beam current. If the beam current decays, the result would be a partial cancellation of the induced fields and therefore a reduction of F_z. Collisional decay of the beam current will be too slow to be important. However, beam electron loss during its propagation could be a significant cause of beam current decay and hence reduce the effectiveness of the trapping mechanism in our discussion. Such consideration leads us to emphasize the $\Omega_e\Omega_i/\nu_e\nu_i$ term in $\nu_\perp$ of Eq. (34). Since this term originates from an efficient decay mechanism (neutralization of δE_r by the ions) unique to the drift angular counter current, it can be adjusted so as to compensate for the negative effect of beam current decay. In reality, when the beam current decay becomes nonnegligible, the contribution from this term may very well be the deciding factor for efficient beam retardation.

In the Cornell astron experiment, a neutral background gas of several hundred microns had to be used for sufficiently rapid plasma generation. At this pressure ν_e was probably comparable to or even much greater than Ω_e, thus only an insignificant part of the observed angular counter current (80% of the beam current was neutralized[26]) could be of the drift type, while most part of it was of the resistive type (i e., $\delta J_\theta = \sigma \delta E_\theta$) . Therefore, the relatively low trapping efficiency (1–10%) as observed in their experiment may be attributable to the absence of the drift current decay mechanism described here. If this was indeed the case, better trapping efficiency should be obtainable by preionizing the plasma to the conditions, Eq. (14), suitable for drift current induction.

VI. ENERGY TRANSFER PROCESSES—PLASMA HEATING

We shall now look into the various mechanisms through which the beam loses its axial energy, and show that the total energy is conserved. For clarity, the skin depth effects, which are of secondary importance in the discussions to follow, will again be neglected. All the expressions to be derived in this section apply to the region occupied by the beam.

The loss rate for beam axial energy density, denoted by P_b, can be obtained from Eqs. (31a,b,c)

$$P_b = n_b F_z v_0 \approx \frac{m n_b^2 a^2}{n_0 (a^2 + \lambda^2)} \left[\nu_e v_0^2 \exp\left(\frac{Z}{l_\parallel}\right) + r^2\omega^2 \nu_\perp \exp\left(\frac{Z}{l_\perp}\right) \right]. \tag{35}$$

The axial plasma current δJ_z driven by δE_z is producing Ohmic heat at the rate

$$P_{\parallel e} = \delta J_z \delta E_z \approx \frac{m n_b^2 a^2 v_0^2 \nu_e}{n_0 (a^2 + \lambda^2)} \exp\left(\frac{2Z}{l_\perp}\right) = \frac{a^2}{a^2 + \lambda^2} \eta \delta J_z^2, \tag{36}$$

where $\eta = m\nu_e/(n_0 e^2)$ is the scalar resistivity of the plasma for current flowing parallel to the magnetic field.

Apart from the exponential factor, $P_{\parallel e}$ is identical to the first term of Eq. (35). We shall show later that the difference goes into the magnetic field associated with the gradually emerging net axial current.

In order to account for the second term of Eq. (35), it is necessary to calculate $\delta \mathbf{v}_e$ and $\delta \mathbf{v}_i$ separately. These two quantities can be formally obtained from the basic equations in the same manner as the other quantities. Alternatively, the mobility tensors, as shown in Appendix D, will yield $\delta \mathbf{v}_e$ and $\delta \mathbf{v}_i$ to our order of approximation. Insofar as $\delta \mathbf{E}$ is known, the alternative method will be used. Thus,

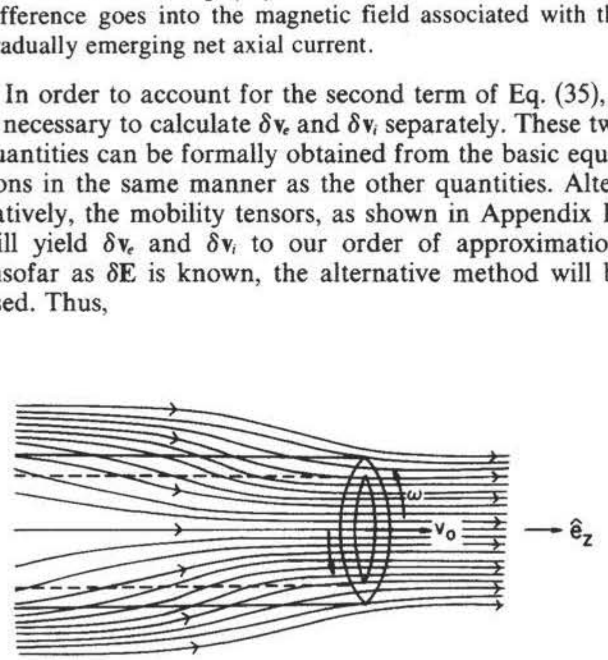

FIG. 5. Magnetic field lines are pushed out of the beam as the unneutralized diamagnetic beam angular current increases spatially away from the beam front.

$$\delta v_{er} = \mu_{err}\,\delta E_r + \mu_{er\theta}\,\delta E_\theta \approx [n_b r \omega \Omega_i a^2/n_0 \nu_i (a^2+\lambda^2)] \exp(Z/l_\perp), \quad (37a)$$

$$\delta v_{e\theta} = \mu_{e\theta r}\,\delta E_r + \mu_{e\theta\theta}\,\delta E_\theta \approx (n_b r\omega/n_0) \exp(Z/l_\perp), \quad (37b)$$

$$\delta v_{ir} = \mu_{irr}\,\delta E_r + \mu_{ir\theta}\,\delta E_\theta \approx (n_b r \omega \Omega_i/n_o \nu_i) \exp(Z/l_\perp), \quad (37c)$$

$$\delta v_{i\theta} \approx 0. \quad (37d)$$

It should be pointed out that δV_{er} and δV_{ir}, although approximately equal, are of entirely different origins. δV_{er} is the $\mathbf{E}\times\mathbf{B}$ drift velocity, but δV_{ir} is driven by δE_r.

From Eqs. (37), we obtain the power dissipated through the cross field current of plasma electrons

$$P_{\perp e} = -n_0 e(\delta v_{er}\,\delta E_r + \delta v_{e\theta}\,\delta E_\theta) = \frac{m n_b^2 r^2 \omega^2 a^2 \nu_e}{n_0(a^2+\lambda^2)} \exp\left(\frac{2Z}{l_\perp}\right) = \frac{a^2}{a^2+\lambda^2}\eta\,\delta J_\theta^2 \quad (38)$$

and the power dissipated through the radial ion current. (Note that $P_{\perp e}$ (or $P_{\parallel e}$) $\propto \nu_e$, but $P_{\perp i} \propto \nu_i^{-1}$. The reason is that $P_{\perp e}$ (or $P_{\perp e}$) results from a nearly constant current δJ_θ (or δJ_z) in the plasma, while $P_{\perp i}$ results from a nearly constant electric field, δE_r, in the plasma.)

$$P_{\perp i} = n_0 e \delta v_{ir}\,\delta E_r, \approx (m n_b^2 r^2 \omega^2 \Omega_e \Omega_i/n_0 \nu_i) \exp(2Z/l_\perp), = (m\Omega_e\Omega_i/n_0 e^2 \nu_i)\,\delta J_\theta^2. \quad (39)$$

Again, apart from the exponential factor and an order (λ^2/a^2) term, the sum of $P_{\perp e}$ and $P_{\perp i}$ is precisely the second term of Eq. (35). As before, the difference due to the exponential factors becomes magnetic field energy.

$P_{\perp e}$ apparently represents the Ohmic power generated by δJ_θ, while $p_{\perp i}$, which feeds energy to the ions, involves the following process. To begin with, ions are accelerated radially by δE_r with a tendency to neutralize the space charge, to which the magnitude of both δE_r and δJ_θ are proportional. As δJ_θ thus decays, δE_θ and δB_r will be induced, Eqs. (27) and (28). δE_θ causes the electrons to drift radially against δE_r (at the expense of beam axial energy) so as to oppose the space charge neutralization and maintain the strength of δE_r. Meanwhile, δB_r will produce a retarding force on the beam, Eq. (31c), and thereby extract its energy. (The energy gained here becomes the work done in the last process.) The over-all result is that ions continuously gain energy from the electric field energy, $\delta E_r^2/8\pi$, which is simultaneously replenished with the beam axial energy through the actions of δE_θ and δB_r.

To show the conservation of energy, we denote the fraction of P_b that goes into beam self-magnetic field energy by P_m. From Eqs. (35), (36), (38), and (39), we obtain

$$P_m = P_b - P_{\parallel e} - P_{\perp e} - P_{\perp i},$$

$$\approx \frac{m n_b^2 a^2}{n_0(a^2+\lambda^2)} \left\{ \nu_e v_0^2 \exp\left(\frac{Z}{l_\parallel}\right)\left[1-\exp\left(\frac{Z}{l_\parallel}\right)\right] + r^2\omega^2\ \nu_\perp \mathrm{exr}\left(\frac{Z}{l_\perp}\right)\left[1-\exp\left(\frac{Z}{l_\perp}\right)\right]\right\},$$

$$\approx \frac{2\pi a^2}{c^2}\frac{d}{dt}|J_t|^2,$$

where $\mathbf{J}_t = (J_{b\theta}+\delta J_\theta)\hat{e}_\theta + (J_{bz}+\delta J_z)\hat{e}_z$ is the combined beam and plasma current.

Initially, $J_t \approx 0$, so a larger fraction of P_b goes into plasma heat than into magnetic field energy. As J_t grows, the reverse gradually becomes true. It may be deduced that, after δJ finally decays away, the total heat going into the plasma roughly equals the unneutralized self-magnetic field energy of the beam. As noted in Sec. III, however, all our final expressions are valid only for the initial stage where $J_t \le \frac{1}{2}J_b$. It can be shown that δJ

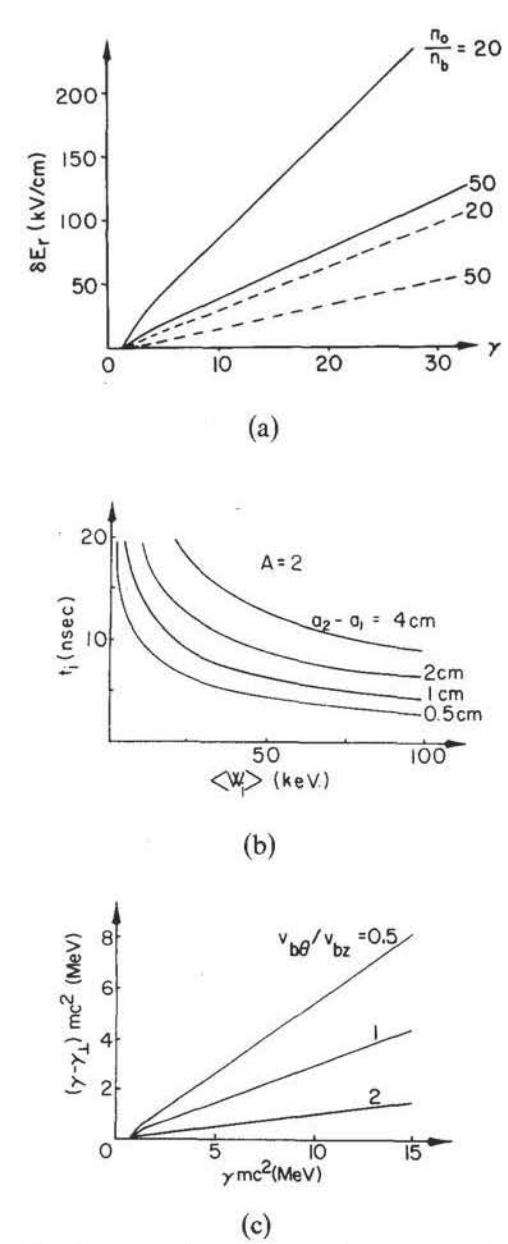

FIG. 6. (a) Plot of Eq. (40) for different parameters. Solid line: $a = 3$ cm. Dashed line: $a = 10$ cm. (b) Plot of deuterium ion heating time vs the average kinetic energy it would reach. Note that t_i is a decreasing function of $\langle W_i \rangle$. (c) Plot of beam electron axial energy vs total energy for different angular to axial velocity ratios.

decays hyperbolically (i.e., $\sim Z^{-1}$), instead of exponentially, at $|Z| \gg l_\perp, l_\parallel$. As a result, the total beam energy loss is infinite, although still equally partitioned between thermal and magnetic field energy. This unphysical situation is apparently created by the inapplicability of the constant velocity beam model at the later stages where the beam should have long been exhausted of its axial energy.

Janes *et al.*[27] proposed a devicc called HIPAC in which ions may be accelerated in a strong electrostatic potential well created by an electron cloud. At Cornell University, the availability of intense relativistic electron beams has led to the study of similar heating methods for plasma ions. The ion heating mechanism in this discussion is electrostatic in nature but features a relatively smaller electric field δE_r capable of self-sustaining. [Because δE_r is associated with δJ_θ, Eq. (22b), its lifetime is considerably lengthened by the inductive effect.]

If δJ_θ in Eq. (23) is approximated by $n_b ec$, δE_r then takes the simple form

$$\delta E_r \approx (n_b/n_0) B_0 .$$

Eliminating B_0 in favor of γ and a by use of Eq. (25), we obtain

$$\delta E_r \approx \gamma n_b mc^2/n_0 ae \approx 500(\gamma n_b/n_0 a) \text{ kV/cm}. \quad (40)$$

Substituting into Eq. (40) the parameters previously used for the Cornell astron experiment, we obtain $\delta E_r \approx 2.2$ kV/cm.

The ion mean free path, d_i, at the assumed pressure (0.5 Torr) is approximately 0.5 cm, so its average kinetic energy, $\langle W_i \rangle$, is $\langle W_i \rangle = \langle \frac{1}{2} M \delta v_i^2 \rangle_{\text{av}} \approx 1.1$ keV.

Ion heating time t_i is approximately

$$t_i \approx [2Md_i/e\delta E_r]^{\frac{1}{2}} \approx \begin{cases} 30 \text{ nsec, for deuterium} \\ 80 \text{ nsec, for nitrogen} \end{cases} .$$

For fully ionized plasmas, d_i increases sharply with the ion energy. Assume $d_i \gtrsim a_2 - a_1$, a rough estimate of $\langle W_i \rangle$ and t_i is

$$\langle W \rangle \approx \tfrac{1}{2}(a_2 - a_1)\delta E_r$$

$$t_i \approx \left[\frac{2M(a_2 - a_1)}{e\delta E_r}\right]^{\frac{1}{2}} \approx 32(a_2 - a_1)\left(\frac{A}{\langle W_i \rangle}\right)^{\frac{1}{2}} \text{nsec.} \quad (41)$$

In Eq. (41), a_2 and a_1 are in cm, $\langle W_i \rangle$ in keV, and A is the ion mass number.

Since $\delta E_r \propto \gamma/a$, the ions can attain considerably higher energies if ultrarelativistic electron beams are used. For example, for $\gamma \approx 10$, $a \approx 3$ cm, $n_0 \approx 20 n_b$, and $a_2 - a_1 = 2$ cm

$$\langle W_i \rangle \approx 80 \text{ keV}$$

$$t_i \approx 7 \text{ nsec, for deuterium} .$$

Plots of δE_r and t_i are shown in Figs. 6a and b. It is seen that the heating of ions can be accomplished on an extremely short time scale—an important advantage considering the short duration of the beam.

The beam electron axial energy is shown in Fig. 6c as a function of its total energy and angular to axial velocity ratio.

It should be noted that if the ion thermalization process is too slow, a high ion loss rate may result from their being accelerated toward the wall by δE_r. In applications to the astron machine, the main objective is to achieve beam trapping. Ion loss during the trapping stage should not be a serious problem. A compensating advantage, on the other hand, is gained by beam electrons, for which δE_r provides an electrostatic potential well, hence is expected to produce stabilizing effects.

For heating oriented experiments, directed ion velocity may be deflected by a strong applied magnetic field as well as by collisions. For example, the gyro-radius of a 50-keV deuterium ion in a 10-kG field is about 4.6 cm, therefore accelerated ions will mostly turn around before hitting the wall.

An experimental verification of the theory can be performed with only minor modifications of the existing intense relativistic electron beam facilities.

A crude design is shown in Figs. 7a and b to relate the theory to practical laboratory parameters. The first stage is to produce a rotational beam from a nonrotational one by passing it through a cusp magnetic field. The second stage is intended specifically for electrostatic heating of ions by making use of the drift angular counter current. By the time the beam reaches the right-hand magnetic mirror end, it would have lost most of its axial energy to the plasma. Reflection from this mirror end is desirable but not necessary, for heating purposes.

For the parameters shown in Fig. 7a and initially assuming $T_e \gtrsim T_i \approx 1$ eV, the conditions in Eq. (14) are then satisfied:

$$\Omega_e(\approx 1.1 \times 10^{11}) \gg \nu_e(\lesssim 1.1 \times 10^{10}),$$

$$\Omega_i(\approx 2.9 \times 10^{7}) \ll \nu_i(\approx 1.8 \times 10^{8}), \quad \text{for deuterium,}$$

where ν_e and ν_i are based on Coulomb collisions. Consequently, the results derived in this section are applicable which indicate that in 8.5 nsec, an annular hot ion region with an average energy of 60 keV will be created in the plasma. This hot ion region then quickly heats the rest of the plasma. The total energy absorbed by ions during this period is

$$n_0\langle W_i \rangle \approx 1 \text{ J/cm}^3$$

and the available beam energy, calculated from Eqs. (32a,b), is

$$n_b(\gamma - \gamma_\perp)mc^2 \approx 1.4 \text{ J/cm}^3 .$$

The accurate values of ν_e and ν_i are hard to estimate, nevertheless, they play a significant role. To allow this uncertainty, the plasma density (or the mixture of plasma and neutrals) should be controllable so that the condition (14) could be reached. The same is true for astron type experiments for which beam trapping is emphasized.

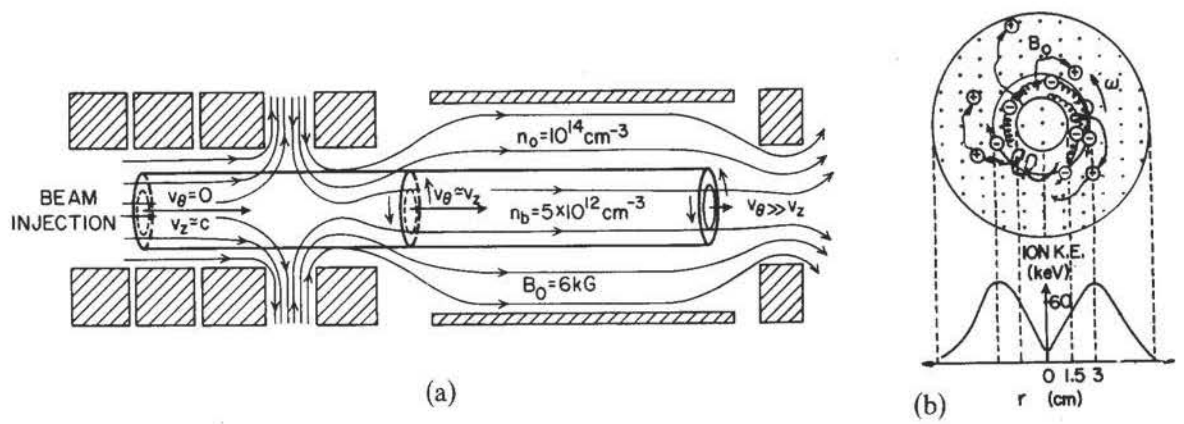

FIG. 7. (a) An experimental design for plasma heating by an intense relativistic electron beam ($I_b = 500$ kA, $\gamma = 12$). (b) Cross-section view. Fig. 7(a). Upper: some plasma particle trajectories. Lower: radial distribution of ion kinetic energies.

VII. DISCUSSION

We have presented a theory which starts with a cold plasma and ends up with a plasma many keV hot. Needless to say, our lowest order theoretical treatment will break down at some point in the time development. We have assumed constant collision frequencies and, by the use of linearized cold plasma fluid equations, we have also neglected the thermal effect, finite ion gyro-radius effect, and the effect of the perturbed magnetic field, etc. Simple as it is, this picture is nevertheless fully self consistent during the initial stage of the interaction when the plasma is still cold and the beam is substantially charge and current neutralized.

The question is then: "to what extent will the beam and plasma interact the way as predicted before any of the unaccounted-for phenomena set in to destroy the subsequent processes?" To answer this question quantitatively, one has to go through considerably more complicated work. Therefore, for the moment, we will content ourselves with some qualitative considerations.

In our description, the plasma particles are continuously flowing out of the beam regions, Eqs. (37a) and (c). If this goes on indefinitely, there will apparently be the problem of plasma depletion. However, the desired effects (beam retardation and plasma heating, etc.) take place so fast that they can normally be accomplished in about 10 nsec. On this time scale, the amount of plasma inside the beam shell ($r < a_1$) will be sufficient to supply the radial flow. Furthermore, the plasma drain inside the shell can later be replenished by the plasma drawn in axially from the open ends.[28] (Note that the beam length is finite in reality.)

Thermal effects have been neglected throughout because generally one would not expect them to play a role comparable to δE_r, which is many kV/cm in amplitude, until the plasma reaches a temperature of as many keV.

In the framework of fluid formulation, we argued that a net electron drift current would be induced if $\Omega_e \gg \nu_e$ and $\Omega_i \ll \nu_i$. The latter condition may seem to be a serious limitation, especially for hot plasmas; however, in the framework of Vlasov formulation, which takes into account the finite ion gyro-radius effects, one would expect this condition to be replaced by an alternative but much less restrictive one, namely,

$$\text{ion gyro-radius} \geq a_2 - a_1. \tag{42}$$

Under this last condition, the ion gyrational and precessional motion would be strongly impeded by the lack of physical space just as they would be impeded by collisions under the condition $\Omega_i \ll \nu_i$. Furthermore, condition (42) would almost certainly hold for general experimental conditions; therefore, by imposing the collisional ion condition ($\Omega_i \ll \nu_i$) in the fluid approach, one has, in fact, to a large extent taken care of the essential physical consequence of finite ion gyro-radius effects.

Finally, let us consider the effects due to time variations of collision frequencies. Angular current neutralization takes place on a time scale of Ω_e^{-1}. Thereafter, the plasma begins to heat up rapidly and the ions become less and less collisional. Eventually, the condition $\Omega_i \ll \nu_i$ breaks down. This development, however, is not expected to change the present results significantly, since we just argued that this condition was more of a special assumption to account for the finite ion gyro-radius effects

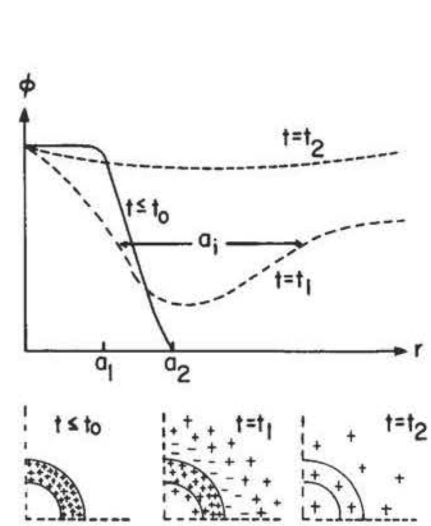

FIG. 8. Calculated space charge and potential distribution ($t \leq t_0$) and conjectured development of them at later times ($t = t_1, t_2$). $t_0 < t_1 < t_2$, $a_i =$ ion gyro-radius.

(which is not inherent in the fluid approach) than a stringent requirement for the existence of drift counter current. On the other hand, as we see from Eq. (39), the increase in plasma temperature (or the decrease in ion collision frequency) is, in fact, a constructive development in the sense that it will result in enhanced ion heating. In this sense also, the electrostatic ion heating mechanism in our discussion is complementary to the usual Ohmic heating mechanism for electrons, Eqs. (36) and (38), whose efficiency decreases drastically as the plasma temperature increases. As a third consequence of the decrease of collision frequencies, the ion thermalization process may become so slow that the ions possess a radially directed gross velocity just as they emerge from the beam outer boundary. As a result, electrons and ions are likely to separate ending up with the streaming ion energy converted back into electric field energy again. The width of the potential well thus formed will approximately be the ion gyro-radius, which is the distance a collisionless ion can travel in the radial direction (Fig. 8, $t = t_1$). The eventual disappearance of the potential well (Fig. 8, $t = t_2$) will be accompanied by further plasma heating, possibly through ion hybrid oscillations or instability induced anomalous phenomena.

ACKNOWLEDGMENTS

We wish to thank the following for discussions and criticisms during the course of this research: Professor R. N. Sudan, Professor G. Benford, Professor R. V. Lovelace, Dr. I. Nebenzahl, Dr. R. Sprangle, and Dr. L. E. Thode on beam theories; Professor J. A. Nation, Professor B. Kusse, Dr. D. A. Phelps, Dr. G. D. Mexiel Jr., and Dr. H. Davitian on beam experiments.

This work was supported by the United States Atomic Energy Commission, and based on part of a thesis submitted by one of us (KRC) to Cornell University in partial fulfillment of the requirements for the Ph.D. degree.

APPENDIX A

$$\sigma_{11} = [\omega_p^2/k^2 v_0^2 \Delta(s)] \{-k^2 v_0^2 (s-\nu_e)(s-\nu_i)[(s-\nu_e)(s-\nu_i) + \Omega_e\Omega_i] + \Omega_e^2 s^2[(s-\nu_i)^2 + \Omega_i^2]\},$$

$$\sigma_{22} = [-\omega_p^2/k^2\Delta(s)]\{k^2(s-\nu_e)(s-\nu_i) [(s-\nu_e)(s-\nu_i)+\Omega_e\Omega_i] + k_\perp^2\Omega_e^2[(s-\nu_i)^2+\Omega_i^2]\},$$

$$\sigma_{33} = [-\omega_p^2/\Delta(s)](s-\nu_e)(s-\nu_i)[(s-\nu_e)(s-\nu_i)+\Omega_e\Omega_i],$$

$$\sigma_{12} = \sigma_{21} = [i/k^2 v_0 \Delta(s)]k_\perp \omega_p^2 \Omega_e^2 s[(s-\nu_i)^2+\Omega_i^2],$$

$$\sigma_{13} = -\sigma_{31} = [1/k\Delta(s)]k_\perp \omega_p^2\Omega_e(s-\nu_e)(s-\nu_i)^2,$$

$$\sigma_{23} = -\sigma_{32}[i/kv_0\Delta(s)]\omega_p^2\Omega_e s(s-\nu_e)(s-\nu_i)^2,$$

where

$$\Delta(s) = 4\pi(s-\nu_e)[(s-\nu_e)^2+\Omega_e^2] [(s-\nu_i)^2+\Omega_i^2],$$

$$k^2 = k_\perp^2 - s^2/v_0^2, \quad \omega_p^2 = 4\pi n_0 e^2/m.$$

APPENDIX B

$$\alpha_{11} = s\omega_p^2\{k^2(s-\nu_e)(s-\nu_i)[(s-\nu_e)(s-\nu_i)+\Omega_e\Omega_i] - v_0^{-2}\Omega_e^2 s^2[(s-\nu_i)^2+\Omega_i^2]\} + k^2 s^2(s-\nu_e)[(s-\nu_e)^2+\Omega_e^2][(s-\nu_i)^2+\Omega_i^2],$$

$$\alpha_{22} = s\omega_p^2\{k^2(s-\nu_e)(s-\nu_i)[(s-\nu_e)(s-\nu_i)+\Omega_e\Omega_i] + k^2\Omega_e^2[(s-\nu_i)^2+\Omega_i^2]\} + k^2c^2(s-\nu_e)[(s-\nu_e)^2+\Omega_e^2][(s-\nu_i)^2+\Omega_i^2] \times [k_\perp^2 - s^2\gamma_0^{-2}v_0^{-2}],$$

$$\alpha_{33} = k^2\omega_p^2 s(s-\nu_e)(s-\nu_i)[(s-\nu_e)(s-\nu_i)+\Omega_e\Omega_i] + k^2c^2(s-\nu_e)[(s-\nu_e)^2+\Omega_e^2][(s-\nu_i)^2+\Omega_i^2] \times [k_\perp^2 - s^2\gamma_0^{-2}v_0^{-2}],$$

$$\alpha_{12} = \alpha_{21} = -ik_\perp v_0^{-1}\omega_p^2\Omega_e^2 s^2[(s-\nu_i)^2+\Omega_i^2],$$

$$\alpha_{13} = -\alpha_{31} = -kk_\perp\omega_p^2\Omega_e s(s-\nu_e)(s-\nu_i)^2,$$

$$\alpha_{23} = -\alpha_{32} = -ik_\perp v_0^{-1}\omega_p^2\Omega_e s^2(s-\nu_e)(s-\nu_i)^2,$$

where

$$\gamma_0 = (1 - v_0^2/c^2)^{-1/2}.$$

APPENDIX C

$$W_\theta(k_\perp, s, r') = [ks(\boldsymbol{\sigma}\cdot\boldsymbol{\kappa})_{31} + ikk_\perp v_0(\boldsymbol{\sigma}\cdot\boldsymbol{\kappa})_{32}]J_0(k_\perp r') - k^2(\boldsymbol{\alpha}\cdot\boldsymbol{\kappa})_{33}r'\omega J_1(k_\perp r'),$$

$$W_z(k_\perp, s, r') = [s^2 v_0^{-1}(\boldsymbol{\sigma}\cdot\boldsymbol{\kappa})_{11} + ik_\perp s(\boldsymbol{\sigma}\cdot\boldsymbol{\kappa})_{12} + ik_\perp s(\boldsymbol{\sigma}\cdot\boldsymbol{\kappa})_{21} - k^2 v_0(\boldsymbol{\sigma}\cdot\boldsymbol{\kappa})_{22}]J_0(k_\perp r') - [sv_0^{-1}(\boldsymbol{\sigma}\cdot\boldsymbol{\kappa})_{13} + ik_\perp(\boldsymbol{\sigma}\cdot\boldsymbol{\kappa})_{23}]kr'\omega J_1(k_\perp r'),$$

$$X_r(k_\perp, s, r') = [-k_\perp s\kappa_{11} - i(s^2v_0^{-1} + k_\perp^2 v_0)\kappa_{21} + k_\perp s\kappa_{22}]J_0(k_\perp r') + [isv_0^{-1}\kappa_{23} + k_\perp\kappa_{13}]kr'\omega J_1(k_\perp r'),$$

$$X_z(k_\perp, s, r') = [s^2v_0^{-1}\kappa_{11} + 2iks\kappa_{12} - k^2 v_0\kappa_{22}]J_0(k_\perp r') - [sv_0^{-1}\kappa_{13} + ik_\perp\kappa_{23}]kr'\omega J_1(k_\perp r'),$$

$$X_\theta(k_\perp, s, r') = [ks\kappa_{31} + ikk_\perp v_0\kappa_{32}]J_0(k_\perp r') - k^2 r'\omega\kappa_{33}J_1(k_\perp r')$$

$$Y_z(k_\perp, s, r') = -k_\perp c X_\theta(k_\perp, s, r').$$

APPENDIX D

Using Eqs. (20) in Sec. III, we can show that terms on the left-hand side of Eqs. (1) and (2) are of order (λ^2/a^2) compared to those on the right-hand side. To a first approximation, we may neglect them and derive from Eqs. (1) and (2) the mobility tensor for each species of the plasma.

Employing the cylindrical coordinate system for which $\mathbf{B} = B_0\hat{e}_z$, we obtain

$$\delta\mathbf{v}_e = \boldsymbol{\mu}_e\cdot\delta\mathbf{E}$$

$$\delta\mathbf{v}_i = \boldsymbol{\mu}_i\cdot\delta\mathbf{E},$$

where

$$\mu_e = \frac{-e}{m}\begin{bmatrix} \frac{\nu_e}{\nu_e^2+\Omega_e^2} & \frac{-\Omega_e}{\nu_e^2+\Omega_e^2} & 0 \\ \frac{\Omega_e}{\nu_e^2+\Omega_e^2} & \frac{\nu_e}{\nu_e^2+\Omega_e^2} & 0 \\ 0 & 0 & \frac{1}{\nu_e} \end{bmatrix}$$

$$\approx \frac{-e}{m}\begin{bmatrix} \frac{\nu_e}{\Omega_e^2} & \frac{-1}{\Omega_e} & 0 \\ \frac{1}{\Omega_e} & \frac{\nu_e}{\Omega_e^2} & 0 \\ 0 & 0 & \frac{1}{\nu_e} \end{bmatrix}$$

and

$$\mu_i = \frac{e}{M}\begin{bmatrix} \frac{\nu_i}{\nu_i^2+\Omega_i^2} & \frac{\Omega_i}{\nu_i^2+\Omega_i^2} & 0 \\ \frac{-\Omega_i}{\nu_i^2+\Omega_i^2} & \frac{\nu_i}{\nu_i^2+\Omega_i^2} & 0 \\ 0 & 0 & \frac{1}{\nu_i} \end{bmatrix}$$

$$\approx \frac{e}{M\nu_i}\begin{bmatrix} 1 & \frac{\Omega_i}{\nu_i} & 0 \\ \frac{-\Omega_i}{\nu_i} & 1 & 0 \\ 0 & 0 & 1 \end{bmatrix}.$$

The second expressions for μ being valid for the case $\Omega_e \gg \nu_e$ and $\Omega_i \ll \nu_i$.

* Present address: Naval Research Laboratory, Code 7750, Washington, D. C. 20375.

† Present address: Department of Physics, University of California, Irvine, California 92664.

1. A comprehensive survey of intense relativistic electron beam physics is provided by S. Putnam, Defense Nuclear Agency Report DNA 2849F (1972).
2. J. O. Cox and W. H. Bennett, Phys. Fluids **13**, 182 (1970).
3. D. A. Hammer and N. Rostoker, Phys. Fluids **13**, 1831 (1970).
4. G. Benford, D. L. Book, and R. N. Sudan, Phys. Fluids **13**, 2621 (1970).
5. R. Lee and R. N. Sudan, Phys. Fluids **14**, 1213 (1971).
6. A. A. Rukhadze and V. G. Rukhlin, Zh. Eksp. Teor. Fiz. **61**, 177 (1971) [Sov. Phys.—JETP **34**, 93 (1972)].
7. S. E. Rosinskii and A. A. Rukhadze, Zh. Tekh. Fiz. **41**, 2504 (1971) [Sov. Phys.—Tech. Phys. **16**, 1989 (1972)].
8. K. R. Chu and N. Rostoker, Phys. Fluids **16**, 1472 (1973).
9. S. Graybill, J. Uglam, and S. Nablo, Bull. Am. Phys. Soc. **13**, 56 (1968).
10. T. G. Roberts and W. H. Bennett, Plasma Phys. **10**, 381 (1968).
11. M. L. Andrews, H. Davitian, D. A. Hammer, H. H. Fleischmann, J. A. Nation, and N. Rostoker, Appl. Phys. Lett. **16**, 98 (1970).
12. G. Yonas and P. Spence, in *The Record of the Tenth Symposium on the Electron, Ion and Laser Beam Technology*, edited by C. Susskind (San Francisco Press, San Francisco, Calif., 1970), p. 143.
13. L. S. Levine and I. M. Vitkovitsky, Bull. Am. Phys. Soc. **15**, 1401 (1970).
14. M. L. Andrews, J. J. Bzura, H. H. Fleischmann, and N. Rostoker, Phys. Fluids **13**, 1322 (1970).
15. J. Benford and B. Ecker, Phys. Rev. Lett. **26**, 1160 (1971).
16. C. Stallings, S. Shope, and J. Guillory, Phys. Rev. Lett. **28**, 653 (1972).
17. N. C. Christofilos, in *Proceedings of the Second International Conference on the Peaceful Uses of Atomic Energy* (United Nations, Geneva, 1958), Vol. 32, p. 279.
18. S. Yoshikawa, Phys. Rev. Lett. **26**, 295 (1971).
19. M. L. Andrews, H. Davitian, H. H. Fleischmann, B. Kusse, R. E. Kribel, and J. A. Nation, Phys. Rev. Lett. **27**, 1428 (1971).
20. M. Friedman, Phys. Rev. Lett. **24**, 1098 (1970).
21. M. Friedman and P. Sprangle, Plasma Phys. **14**, 207 (1972).
22. N. C. Christofilos, UCRL Reports 8887 and 5617-T (1959).
23. I. Nebenzahl, Plasma Phys. (to be published).
24. R. V. Lovelace and R. N. Sudan, Phys. Rev. Lett. **27**, 1256 (1971).
25. See, for example, I. S. Gradshteyn and I. M. Ryzhik, *Tables of Integrals, Series, and Products* (Academic, New York, 1965), p. 679.
26. H. Fleischmann (private communication).
27. G. S. Janes, R. H. Levy, H. A. Bethe, and B. T. Feld, Phys. Rev. **145**, 925 (1966).
28. This point was suggested by Dr. Sidney Putnam, Physics International Company.